The Israeli Journal of Aquaculture – Bamidgeh • ISSN 0792-156X • IJA.74.2022.1818367, 13 pages
CCBY-NC-ND-4.0 ● https://doi.org/10.46989/001c.55685

Hepatopancreatic transcriptome response of *Penaeus vannamei* to dietary ulvan

Augusto E. Serrano, Jr.[1,2]*, Barry Leonard M. Tumbokon[2]

[1] *Institute of Aquaculture, College of Fisheries and Ocean Sciences, University of the Philippines Visayas, Miagao, Iloilo, Philippines*

[2] *UPV-National Institute of Molecular Biology and Biotechnology, University of the Philippines Visayas, Miagao, Iloilo, Philippines*

(Received Oct 31, 2022; Accepted Nov 07, 2022; Published Nov 16, 2022)

Keywords: dietary ulvan, hepatopancreas, RNA sequencing, transcriptomic analysis, white shrimp

Abstract

The study aimed to determine the effect of feeding dietary ulvan on some genes and pathways of *Penaeus vannamei* juveniles. Feeding a diet containing ulvan at 1.0 g·kg^{-1} resulted in differentially expressed genes (DEGs) between the treatments and the control group. Ulvan resulted in 53 DEGs with 26 up and 27-down-regulated DEGs. The DEGs were immune-related, while several affected the energy and substrate metabolic pathways. Specific genes upregulated were Glycerol-3-phosphate acyltransferase (GPAT) of the glycerolipid synthesis, centrosomal protein 120 involved in cell cycling and other activities, RNA helicase, an enzyme involved in opening up DNA molecules, ATP-binding cassette, TATA-binding protein, taurine transporter, transcriptional enhancer factor (TEF), C-type lectin among others. Down-regulated genes included gamma-crystallin, which acts as molecular chaperones; catenin alpha, which is involved in adhesion complex; dystrophin, which is involved in scaffolding for several signaling molecules; and maintenance muscle integrity, among others. Top DEGs that affected significantly important pathways include TEAD (transcriptional enhancer factor domain), GSK3B (glycogen synthase Kinase 3 beta), SLC6A1 (i.e., solute carrier Family 6 Member 1), and ADCY2, which affected signal transduction, environmental adaptation as well as the endocrine, immune, nervous, and digestive systems. In conclusion, dietary ulvan resulted in the up-regulation of immune-related DEGs, which could probably be used to adapt to unfavorable conditions and also affected some energy and substrate metabolic pathways that could potentially be used to direct the overall metabolism.

* Corresponding author. e-mail: serrano.gus@gmail.com

Introduction

Aquaculture is one of the fastest developing industries globally, and aquaculture production maintains a steady growth trend. Aquaculture practices have changed dramatically over the past few decades to meet the growing market demand, such as adding growth promoters, immune-enhancing factors, and maximizing production through intensification. High-density farming, in the long run, makes infectious diseases increasingly more severe, including infections caused by various pathogens such as bacteria, viruses, and parasites, which negatively affect the growth of aquatic animals. To control aquatic animal diseases and promote growth, a variety of drugs and antibiotics have been used more widely in aquaculture (Keerthisinghe et al., 2020) but have brought many adverse effects on human health and the ecological environment. More recently, researchers have been finding safe and effective alternative ways to maintain growth while enhancing their resistance to pathogens, especially in the aquaculture shrimp industry, which has been problematic in the last decade.

Some macroalgae have been used as immunostimulants since they contain rich sources of structurally diverse bioactive compounds with antibacterial and antiviral activities (Shanmugam & Mody, 2000; Persson et al., 2011). Ulvan is the major water-soluble polysaccharide in Ulvales green seaweed, e.g., *Ulva and Enteromorpha* spp. (Jiao et al., 2011). These sulfated polysaccharides play a critical role in animal physiological functions (Menard et al., 2004). *Enteromorpha intestinalis*, which contains ulvan, is considered a fouling organism and has been used as an indicator of eutrophication (Blomster et al., 1998). Accumulation of these species results in "green tides" (Blomster et al., 2002) and has become a global problem.

We have previously demonstrated that adding dietary ulvan from *Ulva intestinalis* at 1000 $mg \cdot kg^{-1}$ resulted in higher protein deposition in *Penaeus monodon* postlarvae (Serrano & Declarador 2014). Also, dietary ulvan significantly enhanced the immune response indices such as total hemocyte count (THC), respiratory burst activity, and phenoloxidase activity for *Penaeus vannamei* and *Penaeus monodon* (Lauzon and Serrano, 2015). Sea lettuce (*Ulva lactuca*) in meal form could replace 30% soybean meal in the diet of *Penaeus monodon* without adverse effects on the survival rate, specific growth rate (SGR), feed intake (FI), food conversion efficiency (FCR), the protein efficiency ratio (PER), lipid deposition and body composition (Serrano & Santizo, 2014; Serrano et al., 2015). The calculated optimum incorporation of *U. intestinalis* meal in the diet of *Penaeus monodon* was 13.9 to 14.7%; however, up to 21% inclusion level could be made without deleterious effects on growth and efficiency (Serrano & Tumbokon, 2015). As an immunostimulant, it has been demonstrated that adding ulvan at 1000 to 1500 $mg \cdot kg^{-1}$ to the diet of *Penaeus monodon* could stimulate hemocyte degranulation and activate prophenoloxidase to become phenoloxidase (Declarador et al., 2014). The same study conducted a WSSV challenge test in which the shrimp fed the diet containing 1000 $mg \cdot kg^{-1}$ exhibited a significantly prolonged survival and 77% higher THC.

The present study aims to discover how the Pacific white shrimp responds to dietary ulvan from *U. intestinalis* at the molecular level using RNA sequencing as a tool.

Materials and Methods

Experimental animals and sample collection

Shrimps were provided by the Institute of Aquaculture, College of Fisheries and Ocean Sciences, UP Visayas, and were stocked initially in a circular 250-L tank in seawater at 35 ppt. They were acclimated gradually to 25 ppt. After one week, 18 white shrimps (average weight = 4.14 g) were randomly distributed into 9 containers (16-L capacity); 3 containers were randomly assigned to a control or ulvan group, 3 shrimps each. The control group did not contain ulvan, while the ulvan group was fed a basal diet into which 1 g ulvan$\cdot kg^{-1}$ was incorporated (**Table 1**). Shrimps were fed the experimental diets for 30 days. At the experiment's termination, each group's hepatopancreas was taken and stored in RNAlater™ and kept at -20°C until total RNA isolation, which was done within 3 days.

Table 1 Composition of the experimental diets

Ingredients	*Control diet(g)*	*Ulvan diet(g)*
Peruvian fish meal	20.00	20.00
Shrimp meal	34.00	34.00
Soybean meal	21.00	21.00
CMC	3.48	2.48
Vitamin mix	1.00	1.00
Mineral mix	1.00	1.00
BHT	0.02	0.02
Lecithin	0.50	0.50
Cod liver oil	4.00	4.00
Starch	15.00	15.00
Ulvan	0.00	1.0
TOTAL	100.00	100.00

RNA Extraction, cDNA Library Construction, and Sequencing

Total RNA was extracted using Trizol plus reagent kit (Invitrogen, USA) following the manufacturer's instructions. Liver tissue (100 mg of liver tissue from the shrimp samples) was used for the total RNA extraction. RNA quality and quantity were determined through gel electrophoresis (1.2% agarose in 40 mL TAE buffer) and spectrophotometry (OD 260/280). RNA integrity was evaluated by the distinct gel red-stained 28s and 18s ribosomal RNA (rRNA) bands. Optical density ratios close to or equal to 2.0 were selected for subsequent analysis. The RNA samples were then desiccated in a solution of RNAstable® (Biomatrica, San Diego, CA) for 24-h before sending the samples to Novogene Bioinformatics in Beijing, China, for cDNA library construction, RNA sequencing, and bioinformatic analyses. cDNA was purified using AMPure XP beads (Illumina, San Diego, USA) and subjected to end repair, A-tailing, ligation of adapter sequences, and polymerase chain reaction (PCR) enrichment of the purified products to yield the final cDNA library. The cDNA libraries were generated from the three replicates of the control group and three replicates of the ulvan group for sequencing on Hiseq Illumina 4000 platform, generating ~150 bp paired-end reads.

Bioinformatic Analysis

Bioinformatic analysis was done as described by Arinez et al. (2020) and Ping et al. (2018). Briefly, (1) De Novo Transcriptome Assembly using Trinity software. The corset was then further used to perform hierarchical clustering to remove redundancy. The longest transcripts in each cluster were selected to represent a particular unigene. (2) Gene Functional Annotation in which annotation of contigs or genes was done using 7 databases, namely Nr (NCBI non-redundant protein sequences), Nt (NCBI nucleotide sequences), Pfam (Protein family), Swiss-Prot, KOG/COG (Cluster of Orthologous Groups of Proteins, COG; and eukaryotic Orthologous Groups, KOG), GO (Gene Ontology), and KEGG (Kyoto Encyclopedia of Genes and Genome). (3) Gene Expression Analysis*,* in which *de novo* assembled transcriptome was used as the reference sequence for gene expression analysis. (4) Analysis of Differentially Expressed Genes (DEGs) to identify DEGs using DESeq software based on a negative binomial distribution wherein the *p*-values were normalized first using the *q*-value. A q-value <0.05 and |log2 (fold-change)| >1 were set as the threshold to classify significant differential expression; (5) Enrichment Analysis - GO enrichment of DEGs was done using GOseq R packages and KOBAS software for KEGG Pathway Enrichment Analysis.

Results

Transcriptome sequencing and sequence assembly

To identify the genes involved in *P. vannamei's* response to dietary ulvan, we created six *c*DNA libraries from *m*RNAs extracted from the hepatopancreas of shrimp fed a diet containing ulvan and a control diet (no ulvan). For each group, high-throughput RNA sequencing resulted in 39.54-60.09 million paired-end reads (**Table 2**). After filtering for low-quality reads and for adapter sequences, 38.17-58.16 clean reads (96.54-96.79% from raw data) were generated. From the clean data of the six libraries, about 73.79-76.44% of clean sequences were successfully mapped to the entire reference transcriptome (**Table 2**). The assembly was performed using the combined clean reads from the six libraries. *De novo assembly* using the Trinity software produced 107,730 unigenes (including contigs and singletons ranging from 201 to 15,283 bp; **Table 3**), with an average length of 1,049 bp (N50=1681 bp; **Table 4**).

Table 2 Data quality control summary

Sample	Raw Reads	Clean Reads	Clean Bases	Error(%)	Q20(%)	Q30(%)	GC (%)	Total mapped (% of clean data)
Control1	55934030	54470086	8.17G	0.02	95.73	90.16	50.48	75.83
Control2	59303116	57717060	8.66G	0.02	95.76	90.13	50.74	75.36
Control3	49338646	47690638	7.15G	0.02	95.1	88.81	50.78	74.59
Ulvan1	60086682	58160484	8.72G	0.02	95.25	89.14	50.24	73.79
Ulvan2	39534714	38167934	5.73G	0.02	94.87	88.33	50.48	76.39
Ulvan3	44373538	43373008	6.51G	0.02	96.31	90.97	50.53	76.44

Table 3 Overview of the number of transcripts and unigenes in different length intervals

Transcript length interval	200-500bp	500-1kbp	1k-2kbp	>2kbp	Total
Number of transcripts	43028	30700	18757	15283	107768
Number of unigenes	42993	30698	18756	15283	107730

Table 4 Overview of the number of transcripts and unigenes in different length intervals

	Min Length	Mean Length	Median Length	Max Length	N50	N90	Total Nucleotides
Transcripts	201	1049	619	15159	1681	443	118815357
Unigenes	201	1049	619	15159	1681	443	118802818

Functional gene annotation and classification

To annotate assembled unigenes, we performed BLAST against the genetic databases NCBI non-redundant protein database (NR; 38,167 genes were annotated), NCBI non-redundant nucleotide database (18,846 genes were annotated), KOG (21,850 genes were annotated), Swiss-Prot (32,618 genes were annotated), Protein family (36,137 genes were annotated), and GO (36,564 genes were annotated)(**Table 5**).

Table 5 Annotation of identified unigenes against seven public databases.

Database	Number of unigenes	Percentage
Annotated in NR	38,167	35.42
Annotated in NT	18,846	17.49
Annotated in KOG	21,850	20.28
Annotated in SwissProt	32,618	30.27
Annotated in PFAM	36,137	33.54
Annotated in GO	36,564	33.94
Annotated in KOG	18,492	17.16

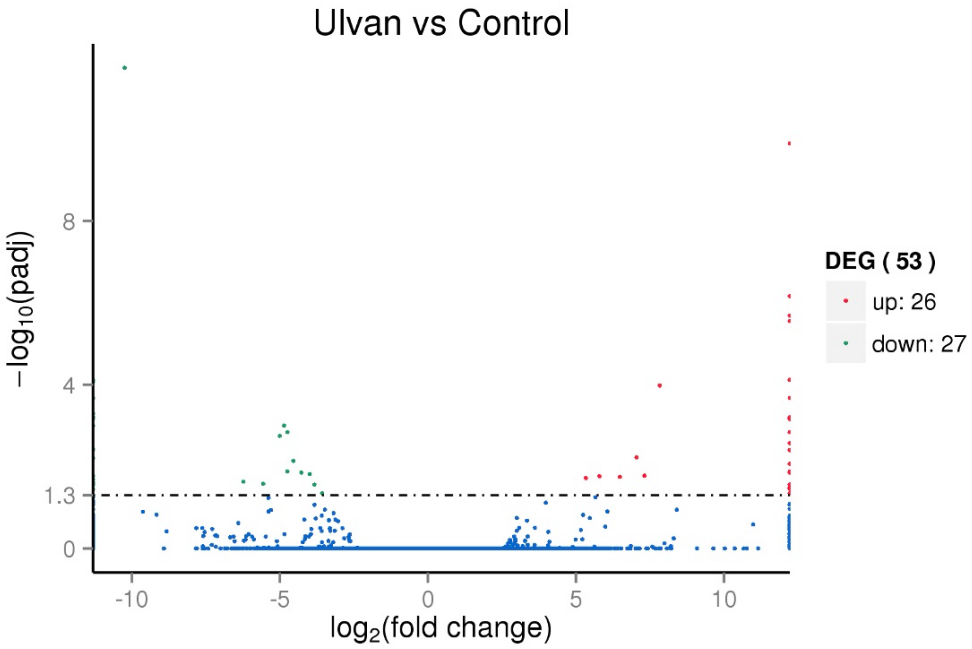

Figure 1 Volcano plot of differentially expressed genes (DEGs) in white shrimp fed the control diet or a diet containing ulvan (1g kg^{-1}). DEGs were selected by padj value <0.05 and $\log_2$ [fold change] > 1. The x-axis shows the fold change in gene expression of the ulvan vs. control groups, and the y-axis shows the statistical significance of the differences. Splashes represent different genes. Red splashes represent significantly up-regulated genes. Green splashes represent significantly down-regulated genes. Blue splashes represent genes without significant differences in expression. The corrected P-value is represented by -log10 (p-adjusted).

Identification of DEGs in Ulvan vs. Control

The volcano plot showing the number and relationship between fold-change and P-value of up- or down-regulated DEGs is shown in **Figure 1**. The ulvan group was compared with the control group; 107,677 unigenes exhibited no significant difference. Feeding diet with ulvan resulted in 26 genes that were significantly up-regulated and 27 unigenes significantly down-regulated.

Table 6 lists the up-regulated and down-regulated genes, respectively. The list of metabolism pathways in **Table 7** shows that the DEGs were immune-related, while some of these DEGs affected the energy and substrate metabolic pathways.

Table 6 Top DEGs, either Up- or down-regulated, involved the comparison of ulvan with the control group

Gene description	Gene ID	FC	pval	Up/down reg
Glycerol-3-phosphate acyltransferase	Cluster-18821.31076	+Inf	2.60E-15	Up
Phosphatase acyltransferase	Cluster-18821.37413	+Inf	2.09E-11	Up
Centrosomal protein of 120 kDa	Cluster-18821.28477	+Inf	5.44E-09	Up
RNA helicase	Cluster-18821.36653	+Inf	6.23E-09	Up
ATP-binding cassette sub-family C	Cluster-18821.38979	+Inf	2.58E-08	Up
TATA-binding protein, TBP	Cluster-18821.17463	+Inf	1.27E-07	Up
RNA cytidine acetyltransferase	Cluster-18821.9404	+Inf	3.16E-07	Up
Taurine transporter	Cluster-18821.37628	+Inf	1.04E-06	Up
Transcriptional enhancer factor	Cluster-18821.18075	+Inf	4.30E-06	Up
C-type lectin 4	Cluster-18821.6697	7.32	6.12E-06	Up
Cuticle protein precursor	Cluster-18821.54923	6.48	7.12E-06	Up
Gamma-crystallin A	Cluster-18821.30188	-10.24	1.85E-17	Down
Organic cation transporter protein	Cluster-18821.29676	- Inf	5.05E-09	Down
Alpha Catenin	Cluster-18821.41773	- Inf	7.79E-09	Down
Protein tyrosine phosphatase receptor type T (PTPRT)	Cluster-18821.42146	-inf	2.43E-08	Down
ATPase	Cluster-18821.53435	-inf	6.79E-08	Down
Dystrophin-like isoform X2	Cluster-18821.18453	-inf	9.27E-08	Down
Ribosomal S6 kinase	Cluster-18821.31321	-inf	1.15E-07	Down
Adducin-related protein	Cluster-18821.28765	-inf	2.07E-07	Down
Survival motor neuron protein (SMN)	Cluster-18821.38009	-4.75	3.25E-07	Down
TLC ATP/ADP transporter	Cluster-18821.40967	-5.00	4.17E-07	Down
E3 ubiquitin-protein ligase	Cluster-18821.38601	-inf	9.63E-07	Down
Phospholipid phosphatase-related protein	Cluster-18821.32502	-inf	1.79E-06	Down
Transporter, ABC superfamily	Cluster-18821.35593	-4.54	2.14E-06	Down
Carbohydrate sulfotransferase	Cluster-18821.36189	-4.75	4.11E-06	Down
Glycogen synthase kinase 3 beta	Cluster-18821.26567	-4.28	4.81E-06	Down
Eukaryotic translation initiation factor	Cluster-18821.45366	-4.00	5.42E-06	Down
Enoyl-CoA hydratase / long-chain 3-hydroxyacyl-CoA dehydrogenase	Cluster-18821.35055	-inf	6.40E-06	Down

Table 7 Metabolism pathways of DEGs involved in the comparison of ulvan with the control group

METABOLISM PATHWAYS	Gene ID	No.of DEGs	padj	Pathway ID	Gene name
Cell growth and death	Cluster-18821.31321 Cluster-18821.43615	2	0.06687627	K04373, K08042	RPS6KA, RSK2 ADCY2
Cellular community - eukaryotes	Cluster-18821.39082 Cluster-18821.41773	2	0.09946589	K05694, K05691	PTPRB, PTPB, CTNNA
Digestive system	Cluster-18821.38979	1	0.20997579	K05665	ABCC1
Signal transduction	Cluster-18821.26567 Cluster-18821.18075 Cluster-18821.41773 Cluster-18821.4428	4	0.00308948	K03083, K09448 K05691 K09448	GSK3B, TEAD CTNNA TEAD
	Cluster-18821.18075 Cluster-18821.4428	2	0.00494938	K09448	TEAD TEAD
	Cluster-18821.18075 Cluster-18821.4428	2	0.04668001	K09448	TEAD TEAD
	Cluster-18821.26567	1	0.15117732	K03083	GSK3B
Translation	Cluster-18821.9404	1	0.25867347	K14521	NAT10, KRE33
Metabolism of cofactors and vitamins	Cluster-18821.26241	1	0.08242329	K00861	RFK, FMN1
Xenobiotics biodegradation and metabolism	Cluster-18821.35055	1	0.07107424	K07515	HADHA
	Cluster-18821.35055	1	0.10471087	K07515	HADHA
	Cluster-18821.35055	1	0.11565268	K07515	HADHA
Lipid metabolism	Cluster-18821.35055	1	0.1389075	K07515	HADHA
	Cluster-18821.35055	1	0.15983527	K07515	HADHA
Carbohydrate metabolism	Cluster-18821.35055	1	0.23392258	K07515	HADHA
	Cluster-18821.35055	1	0.24174391	K07515	HADHA
Amino acid metabolism	Cluster-18821.35055	1	0.29141709	K07515	HADHA
Digestive system	Cluster-18821.43615	1	0.28996032	K08042	ADCY2
	Cluster-18821.43615	1	0.29721461	K08042	ADCY2
Endocrine system	Cluster-18821.31321 Cluster-18821.43615	2	0.050714	K04373, K08042	RPS6KA,RSK2,AD CY2
	Cluster-18821.26567 Cluster-18821.43615	2	0.08448714	K03083, K08042	GSK3B, ADCY2
	Cluster-18821.43615	1	0.23077171	K08042	ADCY2
	Cluster-18821.26567	1	0.27224594	K03083	GSK3B
	Cluster-18821.43615	1	0.30439547	K08042	ADCY2
Environmental adaptation	Cluster-18821.26567	1	0.05184931	K03083	GSK3B
	Cluster-18821.43615	1	0.27522846	K08042	ADCY2
Immune system	Cluster-18821.26567 Cluster-18821.43615	2	0.11979924	K03083, K08042	GSK3B, ADCY2
	Cluster-18821.26567	1	0.21803933	K03083	GSK3B
	Cluster-18821.26567	1	0.29432175	K03083	GSK3B
Metabolism of other amino acids	Cluster-18821.35055	1	0.23706066	K07515	HADHA
Nervous system	Cluster-18821.37628 Cluster-18821.43615	2	0.03185301	K05034, K08042	SLC6A1, ADCY2
	Cluster-18821.26567 Cluster-18821.31321	2	0.08448714	K03083, K04373	GSK3B, RPS6KA, RSK2
	Cluster-18821.43615	1	0.28115719	K08042	ADCY2
	Cluster-18821.31321	1	0.28703788	K04373	RPS6KA, RSK2

GO and KEGG enrichment analysis of DEGs in ulvan vs. control comparison

The rich factor and q-value of KEGG pathways are shown in **Table 8**, where the list of the top 20 pathways that exhibited hits is displayed. On top of the list of down-regulated pathways are the Hippo signaling pathway, endometrial cancer, progesterone-mediated oocyte maturation, circadian rhythm-fly, oocyte meiosis, benzoate degradation, neurotrophin signaling pathway, melanogenesis, and adherens junction. In contrast, the up-regulated pathways were riboflavin metabolism, MAPK signaling pathway-yeast, vitamin digestion and absorption, GABAergic synapse, ribosome biogenesis in eukaryotes, hippo signaling pathway, glycerophospholipid metabolism, ABC transporters, Hippo signaling pathway, and microRNAs in cancer. Interestingly, the Hippo pathway was both a down- and up-regulated pathway as a response to dietary ulvan.

Table 8 Top down-regulated pathways in ulvan vs control group comparison

Pathway term	rich factor	qvalue	Gene no.
Hippo signaling pathway	0.010452962	0.53651046	3
Endometrial cancer	0.012658228	0.53651046	2
Progesterone-mediated oocyte maturation	0.011494253	0.53651046	2
Circadian rhythm - fly	0.040000000	0.53651046	1
Oocyte meiosis	0.009803922	0.53651046	2
Benzoate degradation	0.028571429	0.53651046	1
Neurotrophin signaling pathway	0.008547009	0.53651046	2
Melanogenesis	0.008547009	0.53651046	2
Adherens junction	0.007751938	0.53651046	2
MAPK signaling pathway - yeast	0.020408163	0.53651046	1
Aminobenzoate degradation	0.018867925	0.53651046	1
Chemokine signaling pathway	0.006920415	0.53651046	2
Caprolactam degradation	0.016949153	0.53651046	1
Biosynthesis of unsaturated fatty acids	0.013888889	0.53651046	1
Hedgehog signaling pathway	0.012658228	0.53651046	1
Basal cell carcinoma	0.012195122	0.53651046	1
Fatty acid elongation	0.011904762	0.53651046	1
B cell receptor signaling pathway	0.008403361	0.53651046	1
Ovarian steroidogenesis	0.007874016	0.53651046	1
Propanoate metabolism	0.007751938	0.53651046	1

Table 9 Top up-regulated pathways in ulvan vs control group comparison

Pathway term	rich factor	qvalue	Gene no.
Riboflavin metabolism	0.024390244	0.05712346	1
MAPK signaling pathway - yeast	0.020408163	0.05712346	1
Vitamin digestion and absorption	0.00877193	0.05880254	1
GABAergic synapse	0.007462687	0.05880254	1
Ribosome biogenesis in eukaryotes	0.006896552	0.05880254	1
Hippo signaling pathway - fly	0.006024096	0.05880254	1
Glycerophospholipid metabolism	0.005235602	0.05880254	1
Glycerolipid metabolism	0.004807692	0.05880254	1
ABC transporters	0.003861004	0.06434176	1
Hippo signaling pathway	0.003484321	0.06434176	1
MicroRNAs in cancer	0.002012072	0.0991632	1

To understand the pathways affected by dietary ulvan, **Table 9** shows the degree of enrichment in terms of the Rich factor, q-value, and the number of genes enriched in this pathway. The smaller the q-value, the more significant the enrichment is. The maximum

number of DEGs appeared in the category Hippo signaling pathway; other categories with an equal number of genes were adherens junction, chemokine signaling pathway, GABAergic synapse, hippo signaling pathway-fly, neutrophin signaling pathway.

Discussion

Various investigators have studied the effects of functional feeds in shrimps that enhanced their protection against diseases and environmental stress. For example, Cabrera-Stevens (2021) documented the lowest mortality rate in shrimps fed a diet containing the medicinal plants *Curcuma longa* and *Lepidium meyenni* challenged with WSSV. Their analyses used the transcriptomic comparison of muscle tissues of the various treatments. In the present study, the effects of continued feeding a diet containing ulvan extracted from *Ulva intestinalis* were evaluated, and no challenge with either pathogen or environmental stress was made; the report on the aspect of WSSV challenge test following feeding the ulvan diet is currently being reviewed (Serrano Jr. & Tumbokon, 2022). The effects of dietary ulvan on the treated and non-treated white shrimp's hepatopancreas were made using transcriptomic analysis, the organ being the center of metabolic processes.

Seaweeds have been the focus of recent studies as a rich source of bioactive metabolites with specific nutritional value and therapeutic activities that are very useful in aquaculture. Many sulfated polysaccharides have exhibited antiviral activity against various viruses (Ahmadi et al., 2015). It has also been shown that sulfated polysaccharides from various seaweeds promote the immunostimulation of shrimp challenged with WSSV (Cantelli et al., 2019), and oral administration of diets containing ulvan improve the total hemocyte count and survival of WSSV-infected shrimps (Declarador et al., 2014). In the present study, ulvan supplementation might have induced an immunostimulatory and antioxidant activity that could have enhanced shrimp survival, even perhaps under pathogen or environmental stress.

Identifying genes involved in stress resistance following feeding of functional ingredients such as ulvan is a wise approach in seeking an integral solution to minimize the extreme impact of shrimp diseases and, thus, economic losses. In the present study, we evaluated the differentially expressed genes in shrimp fed a diet containing ulvan. Glycerol-3-phosphate acyltransferase (GPAT) is the rate-limiting enzyme in the *de novo* pathway of glycerolipid synthesis; it catalyzes the conversion of glycerol-3-phosphate and long-chain acyl-CoA to lysophosphatidic acid. In the present study, dietary ulvan up-regulated GPAT 3, which plays a pivotal role in regulating triglyceride and phospholipid synthesis. The implication could be that by regulating *de novo* lipogenesis and lipid efflux, immune cells can be driven from a proinflammatory phenotype to an anti-inflammatory phenotype (Hubler and Kennedy 2016). The helicase gene was also up-regulated by dietary ulvan. Their primary function is to unpackage an organism's genes. They are motor proteins that move directionally along a nucleic acid phosphodiester backbone, separating two annealed nucleic acid strands (i.e., DNA, RNA, or RNA-DNA hybrid) using energy derived from ATP hydrolysis.

In contrast, down-regulated by the dietary ulvan in white shrimp was gamma-crystallin A which comprises the majority of soluble protein in the lens and contributes to the transparency and refractive properties of the lens structure. Gamma-crystallins are differentially regulated after early development and have been involved in cataract formation (Wong et al., 2019). Down-regulation of this gene in the present study indicated normal and healthy conditions of the shrimp’s eye lens. Also, down-regulated was catenin alpha, an essential F-actin-binding protein of the cadherin/catenin adhesion complex involved in cell-cell adhesion. In the absence of α-catenins, different signaling pathways likely converge to stimulate cell cycle activity (Vite et al., 2015), and it is possible that since it was down-regulated in the ulvan group in the present study, cell cycle activity could be partly activated through other signaling pathways. The down-regulated tyrosine phosphatase receptor type T (PTPRT, Table 6) is a signaling molecule regulating various cellular processes, including cell growth, differentiation, mitotic

cycle, and oncogenic transformation. In humans, PTPRT mutation can predict survival benefits from cancer ICI (immune checkpoint inhibitor) therapy; it could be that the down-regulation of this gene in shrimps by feeding ulvan in the present study was somehow beneficial to the health of the shrimps. Another down-regulated gene was dystrophin, a protein that provides a structural link between the muscle cytoskeleton and extracellular matrix to maintain muscle integrity. The final effects of both the WSSV and AHPND infection was an over-expressed dystrophin gene. Thus, the down-regulation of the dystrophin gene in the present study following feeding the ulvan diet was characteristic of a normal and healthy white shrimp.

The Hippo signaling pathway plays a crucial role in organ size control (reviewed by Zhao et al., 2010) and in the development of human cancers (Zhou et al., 2009). This might be due to its ability to regulate cell proliferation and apoptosis or its functions in the renewal and expansion of stem cells and progenitor cells. Organ development is a coordinated process of increased organ size and morphogenesis mediated by extensive crosstalk between signaling pathways. In the present study, this pathway exhibited the most hit; interestingly, it was in the list of up-and-down-regulated genes. Liao et al. (2021) observed that the Hippo signaling pathway fly was one of the top 20 enriched KEGG pathways that responded to the infection of the white spot syndrome virus (WSSV) in *Marsupenaeus japonicus* hepatopancreas. This was also our finding in the hepatopancreas *P. vannamei* infected with WSSV following feeding ulvan (Serrano & Tumbokon, 2022)

The mitogen-activated protein kinase (MAPK) cascade is a highly conserved module involved in various cellular functions. MAPK families are essential in complex cellular programs like proliferation, differentiation, development, transformation, and apoptosis. MAPK pathways relay, amplify and integrate signals from a diverse range of stimuli and elicit an appropriate physiological response (Zhang & Liu, 2002). In the present study, dietary ulvan resulted in the up-regulation of this pathway (**Figure 2**).

The amino acid GABA (γ-aminobutyric acid) acts as an inhibitory neurotransmitter in vertebrate and invertebrate nervous systems. GABA might also act as a trophic substance during nervous system development and regulate neuronal proliferation and migration in the developing cortex (Owens & Kriegstein, 2002). In the present study, the GABAergic synapse pathway was up-regulated as a result of ulvan in the diet of the white shrimp (**Figure 2**)

A down-regulated homolog protein, which belonged to the pathway of endometrial cancer, was catenin (**Figure 2**). This protein functions as a linking protein between cadherins and actin-containing filaments of the cytoskeleton; it is required for maintaining the integrity of the intercellular adherens junction, a cell junction whose cytoplasmic face is linked to the actin skeleton (Sun et al., 2014). Thus, a down-regulated α-catenin can result in loss of cell-cell adhesion, a common characteristic of cancer cells.

Top DEGs that affected significantly important pathways include TEAD (transcriptional enhancer factor domain), GSK3B (glycogen synthase Kinase 3 beta), SLC6A1 (i.e., solute carrier Family 6 Member 1), and ADCY2, which affected signal transduction, environmental adaptation as well as the endocrine, immune, nervous, and digestive systems. The TEAD transcriptional factors bind to a transcriptional coactivator called the Yes-associated protein (Yap) to induce the expression of cell cycle regulators and other target genes mainly controlled by the Hippo pathway. Thus, dietary ulvan resulted in the up-regulation of TEAD genes in the Hippo pathway to regulate organ growth in the white shrimp, as was observed in *Drosophila* and vertebrates (Barry & Camargo, 2013). GSK3B is a protein involved in the signal transmission process related to energy metabolism, exhibited down-regulated phosphorylation in the present study in white shrimp fed with an ulvan-supplemented diet. GSK3B is a protein-serine kinase that was initially characterized as a regulator of glycogen metabolism (Plyte et al., 1992) and is involved in a series of signal transduction pathways that regulate cell growth, differentiation, and development (Siegfried et al., 1990). It phosphorylates and inactivates glycogen synthase, the rate-limiting enzyme of glycogen synthesis (Parker et al., 1983). When an organism is offered food that contains more energy

than it requires, glycolysis is inhibited, and the excess energy is converted into glycogen for storage (Barcellos et al., 2010). The present study indicated that dietary ulvan could refine the control of energy metabolism of *P. vannamei* by inhibiting the phosphorylation of enzymes (i.e., GSK3B) from promoting glycogen synthesis and perhaps also enhanced glycolysis (Mi et al., 2021). SLC6A1 is a gene for protein, a gamma-aminobutyric acid (GABA) transporter that localizes to the plasma membrane and is involved in synaptic signaling (Voisin et al., 2019). The SLC6A1 expression levels are correlated negatively with several significant immune cells (Zhang et al., 2021). ADCY encodes enzymes that catalyze cyclic AMP (cAMP) formation (Honoune & Defer, 2001). cAMP in teleosts induces the initiation of sperm motility in salmonids and the phosphorylation of spermatozoa axonemal proteins in sea bream (Zilli et al., 2009). The up-regulation of ADCY2 in ulvan-treated *P. vannamei* in the present study could indicate the potential positive effects on the male reproductive potential.

In conclusion, dietary ulvan resulted in the up-regulation of immune-related DEGs, which could probably be used to adapt to unfavorable conditions and also affected some energy and substrate metabolic pathways that potentially could be used to direct the overall metabolism.

Acknowledgments

The authors wish to thank the University of the Philippines Visayas for the Leverage Fund it provided to the research project. The authors would like to thank the Philippine Council for Agriculture, Aquatic and Natural Resources Research and Development (PCAARRD) of the Department of Science and Technology (DOST) for the research grant; the Office of the Vice-Chancellor of Research and Extension of the University of the Philippines Visayas for the publication grant, We are also grateful to Mr. Vicente Nim and Ms. Marj Gem Bunda for the technical assistance.

References

Ahmadi, A., Moghadamtousi, S.Z., Abubakar, S., Zandi, K., 2015. Antiviral potential of algae polysaccharides isolated from marine sources: A review. *BioMed Res. Int.* 2015:825203. https://doi.org/10.1155/2015/825203

Barcellos, L.J.G., Marqueze, A., Trapp, M., Quevedo, R.M., Ferreira, D., 2010. The effects of fasting on cortisol, blood glucose and liver and muscle glycogen in adult jundiá *Rhamdia quelen. Aquaculture*, 300: 231-236. https://doi.org/10.1016/j.aquaculture.2010.01.013

Barry, E.R., Camargo, F.D., 2013. The Hippo superhighway: signaling crossroads converging on the Hippo/Yap pathway in stem cells and development. *Current Opinion in Cell Biology*. 25:247–253. https://doi.org/10.1016/j.ceb.2012.12.006

Blomster, J., Maggs, C.A., Stanhope, M.J., 2002. Molecular and morphological analysis of *Enteromorpha intestinalis* and *E. compressa* (Chlorophyta) in the British Isles. *Journal of Phycology* 34(2):319-340. https://doi.org/10.1046/j.1529-8817.1998.340319.x

Blomster, J., Back, S., Fewer, D.P., Kiirikki, M., Lehvo, A., Maggs, C.A., Stanhope, M.J., 2002. Novel morphology in *Enteromorpha* (Ulvophyceae) forming green tides. *Am. J. Bot.* 89(11):1756-63. https://doi.org/10.3732/ajb.89.11.1756

Cabrera-Stevens, M.J., Sanchez-Paz, A., Mendoza-Cano, F., Escobedo-Fregoso, C., Encinas-Garcia, T., Elizondo-Gonzalez, R., Pena-Rodriguez, A., 2022. Transcriptome analysis reveals differential gene expression associated with white spot syndrome virus resistance in the shrimp *Litopenaeus vannamei* fed on functional diets. *Aquaculture* 547, 737434. https://doi.org/10.1016/j.aquaculture.2021.737434

Cantelli, L., Goncalves, P., Guertler, C., Kayser, M., Pilotto, M.R., Barracco, M.A., Perazzolo, L.M., 2019. Dietary supplementation with sulfated polysaccharides from *Gracilaria birdiae* promotes a delayed immunostimulation in marine shrimp challenged by the white spot syndrome virus. *Aquac. Int.,* 27: 349-367. https://doi.org/10.1007/s10499-018-0328-1

Declarador, R.S., Serrano Jr., A.E., Corre, V.L., 2014. Ulvan extract acts as immunostimulant against white spot syndrome virus (WSSV) in juvenile black tiger shrimp *Penaeus monodon. AACL Bioflux* 7: 153-161.

Hanoune, J., N. Defer, N., 2001. Regulation and role of adenylyl cyclase isoforms. *Annu Rev. Pharmacol. Toxicol.,* 41: 145-174. https://doi.org/10.1146/annurev.pharmtox.41.1.145
Hubler, M.J., Kennedy, A.J., 2016. Role of lipids in the metabolism and activation of immune cells. *J. Nutr. Biochem*. 34: 1–7. https://doi.org/10.1016/j.jnutbio.2015.11.002
Jiao, G., Yu, G., Zhang, J., Ewarf, H.S., 2011. Chemical structures and bioactivities of sulfated polysaccharides from marine algae. *Mar. Drugs* 9(2): 196-223. 10.3390/md9020196
Keerthisinghe, T.P., Wang, F., Wang, M., Yang, Q., Li, J., Yang, J., Xi, L., Dong, W., Fang, M., 2020. Long-term exposure to TET increases body weight of juvenile zebrafish as indicated in host metabolism and gut microbiome. *Environ. Int.*, 139, 105705. https://doi.org/10.1016/j.envint.2020.105705
Lauzon Q.D., Serrano Jr., A.E., 2015. Ulvan extract from *Enteromorpha intestinalis* enhances immune responses in *Litopenaeus vannamei* and *Penaeus monodon* juveniles. *ABAH Bioflux* 7(1):1-10.
Liao, M., Zhao, J., He, Z., Chen, X., Xue, Y., Zhou, J., Long, X., Sun, C., 2021. Transcriptome analysis of *Marsupenaeus Japonicus* hepatopancreas during WSSV persistent infection." *Israeli Journal of Aquaculture - Bamidgeh* 73: 1–15. https://doi.org/10.46989/001c.27662.
Menard, R., Alban, S., De Ruffray, P., Jamois, F., Franz, G., Fritig, B., Yvin, J. C., Kauffman, S., 2004. β-1,3 glucan sulfate, but not β-1,3 glucan, induces the salicylic acid signaling pathway in tobacco and arabidopsis. *Plant Cell* 16:3020-2032. https://doi.org/10.1093/jxb/erm008
Mi, R., Rabbi, M.H., Sun, Y., Li, X., Ma, S., Wen, Z., Meng, N., Li, Y., Du, X., Li, S., 2021. Enhanced protein phosphorylation in *Apostichopus japonicus* intestine triggered by tussah immunoreactive substances might be involved in the regulation of immune-related signaling pathways. *Comp. Biochem. Physiol., D: Genomics and Proteomics* 37, 100757. https://doi.org/10.1016/j.cbd.2020.100757
Owens, D.F., Kriegstein, A.R., 2002. Is there more to GABA than synaptic inhibition? Nature Reviews: Neuroscience 3: 715-727. https://doi.org/10.1038/nrn919
Parker, P.J., Caudwell, F.B., Cohen, P., 1983. Glycogen synthase from rabbit skeletal muscle: effect of insulin on the state of phosphorylation of the seven phosphoserine residues in vivo. *Eur. J. Biochem.,* 130: 227-234. https://doi.org/10.1111/j.1432-1033.1983.tb07140.x
Persson, F., Svensson, R., Fredriksson N.J., Pavia, H., Hermansson, M., 2011. Ecological role of a seaweed secondary metabolite for a colonizing bacterial community. *Biofouling* 27: 579–588. https://doi.org/10.1080/08927014.2011.589001
Ping, W., L. Yudong, C. Shuai, and G. Fukun. 2018. Hepatic transcriptome profiling under shear stress in *Sciaenops ocellatus*. Israeli Journal of Aquaculture - Bamidgeh 70. 1469. 10 pages. https://doi.org/10.46989/001c.20934
Plyte, S.E., Hughes, K., Nikolakaki, E., Pulverer, B.J., Woodgett, J.R., 1992. Glycogen synthase kinase-3: functions in oncogenesis and development. BBA-Rev Cancer, 1114: 147-162. https://doi.org/10.1016/0304-419X(92)90012-N
Serrano Jr., A.E., Declarador, R.S., 2014. Growth performance of black tiger shrimp *Penaeus monodon* larvae fed diets supplemented with ulvan. *ABAH Bioflux* 6(2):173-180.
Serrano Jr., A.E., Santizo, R., 2014. Dietary substitution of protein concentrate of *Ulva lactuca* for soybean meal in the black tiger shrimp *Penaeus monodon* fry. *ABAH Bioflux* 6(2):140-147.
Serrano Jr., A.E., Tumbokon, B.L.M., 2015. Optimum dietary inclusion of *Ulva intestinalis* to the diet of the black tiger shrimp Penaeus *monodon* postlarvae. *ABAH Bioflux 7(2):169-176.*
Serrano Jr., A.E., Tumbokon, B.L.M., 2022. Transcriptome profiling of *Penaeus vannamei* hepatopancreas infected with WSSV following feeding diet containing ulvan. *Israeli Journal of Aquaculture - Bamidgeh* 74: 1–14. https://doi.org/10.46989/001c.40365
Serrano Jr., A.E., Declarador, R.S., Tumbokon, B.L.M., 2015. Proximate composition and apparent digestibility coefficient of *Sargassum* spp. meal in the Nile tilapia, *Oreochromis niloticus*. *ABAH Bioflux* 7(2):159-168.
Shanmugam, M., Mody, K.H., 2000. Heparinoid-active sulphated polysaccharides from marine algae as potential blood anticoagulant agents. *Current Science* 79(12): 1672-1683.
Siegfried, E., Perkins, L., Capaci, T., Perrimon, N., 1990. Putative protein kinase product of the Drosophila segment polarity gene, zeste- white 3. *Nature* 354, 825-829. https://doi.org/10.1038/345825a0
Sun, Y., Zhang, J., Ma, L., 2014. α-Catenin: a tumor suppressor beyond adherens junctions. *Cell Cycle* 13(15): 2334-2339. https://doi.org/10.4161/cc.29765

Vite, A., Li, J., Radice, G.L., 2015. New Functions for alpha-catenins in Health and Disease: From Cancer to Heart Regeneration. *Cell Tissue Res.* 2015 Jun; 360(3): 773–783. https://doi.org/10.1007/s00441-015-2123-x

Voisin, A. S., Kültz, B., Silvestre, F., 2019. Early-life exposure to the endocrine disruptor 17-α-ethinylestradiol induces delayed effects in adult brain, liver and ovotestis proteomes of a self-fertilizing fish. *J. Proteomics* 194: 112-124. https://doi.org/10.1016/j.jprot.2018.12.008

Wong, E.K., Prytkova, V., Freites, J.A., Butts, C.T., Tobias, D.J., 2019. Molecular mechanism of aggregation of the cataract-related γD-crystallin W42R variant from multiscale atomistic simulations. *Biochemistry* 58:3691–3699. https://doi.org/10.1021/acs.biochem.9b00208

Zhang, W., Liu, H.T., 2002. MAPK signal pathways in the regulation of cell proliferation in mammalian cells. *Cell Research* 12: 9-18. https://doi.org/10.1038/sj.cr.7290105

Zhang, D.D., Wang, W.E., Ma, Y.S., Shi, Y., Yin, J., Liu, J.B., Yang, X.L., Xin, R., Fu, D., Wen-Jie Zhang, W.J., 2021. A miR-212-3p/SLC6A1 regulatory sub-network for the prognosis of hepatocellular carcinoma. *Cancer Manag. Res.,* 13:5063-5075. https://doi.org/10.2147/CMAR.S308986

Zhao, B., Li, L., Guan, K.L. 2010. Hippo signaling at a glance. *Journal of Cell Science* 123: 4001-4006. https://doi.org/10.1242/jcs.069070

Zhou, D., Conrad, C., Xia, F., Park, J.S., Payer, B., Yin, Y., Lauwers, G.Y., Thasler, W., Lee, J.T., Avruch, J., Bardeesy, N., 2009. Mst1 and Mst2 maintain hepatocyte quiescence and suppress hepatocellular carcinoma development through inactivation of the Yap1 oncogene. *Cancer Cell* 16: 425-438. https://doi.org/10.1016/j.ccr.2009.09.026

Zilli, L., Schiavone, R., Storelli, C., Vilella, S., 2008. Molecular mechanisms determining sperm motility initiation in two sparids (*Sparus aurata* and *Lithognathus mormyrus*). *Biology of Reproduction* 79: 356–366. https://doi.org/10.1095/biolreprod.108.068296